Nonradiative decay processes of 4*d* hole states in CsF, BaF_2, and LaF_3

Kouichi Ichikawa, Osamu Aita, and Katsuhito Aoki
College of Engineering, University of Osaka Prefecture, Mozu-Umemachi, Sakai, Osaka 591, Japan

Masao Kamada
Institute for Molecular Science, Okazaki, Aichi 444, Japan

Kenjiro Tsutsumi
Faculty of Engineering, Setsunan University, Ikeda-Nakamachi, Neyagawa, Osaka 572, Japan
(Received 23 August 1991)

The nonradiative decay of 4*d* hole states in CsF, BaF_2, and LaF_3 was investigated by photoelectron spectroscopy with synchrotron radiation. The $N_{4,5}O_{2,3}O_{2,3}$ Auger peak is resonantly enhanced around an energy region of 4*d* excitation of cations. Constant-final-state spectra with the final state at this Auger peak agree well in shape and in energy with respective absorption features. Intensities of 5*s* and 5*p* electrons of cations are also resonantly enhanced around the absorption features, while the valence band does not show any enhancement except for LaF_3. The spectral shape of constant-initial-state (CIS) spectra with initial states at 5*s* and 5*p* levels is different from the absorption features. In particular, intensities of both CIS spectra decrease rapidly relative to their corresponding total photoelectric yield spectra in the higher-energy region. From these results, we propose that 4*d* hole states decay predominantly through the $N_{4,5}O_{2,3}O_{2,3}$ Auger process and the direct-recombination processes are suppressed in the higher-energy region. It was also found that the photoemission branching ratio of $5p_{1/2}$ to $5p_{3/2}$ levels of BaF_2 and LaF_3 changes drastically at excitation photon energy of the $^3D_1$ state. It is attributed to a difference in the *p-d* interaction between the $5p_{1/2}$ and $5p_{3/2}$ hole states at the photoemission final state.

I. INTRODUCTION

There have been many studies on the absorption spectra of rare earths and Xe-like ions in the energy region of 4*d* excitation.[1-14] The absorption spectra show weak lines with widths of several tenths of an eV and giant peaks with widths ranging from 15 to 70 eV. The former for rare earths has been attributed to multiplet structures due to the $4d^9 4f^{n+1}$ states within an atomic picture (n is the number of 4*f* electrons in the ground state), while the latter is explained in terms of configuration interactions between $4d^9 4f^{n+1}$ multiplet states and the continuum.[15-17] On the other hand, the absorption spectra of Xe-like ions such as Cs^+ and Ba^{2+} have been interpreted in terms of the effective potential for *f* orbits, which has a double-well structure.[13,18,19] An inner well is separated from the outer one by a potential barrier. Along the isoelectronic sequence, the inner well becomes deeper and deeper as nuclear charge increases and leads to sudden collapse of the 4*f* orbit from the outer into the inner well. Thus the giant absorption peaks are interpreted in terms of delayed onsets of 4*d*-*f* transitions within an atomic picture. However, experimental studies on various states of barium[12-14] and theoretical study on some cerium compounds[20] show that sharp lines and giant peaks are sensitive to the valency and the crystal structure. Thus absorption structures are not completely interpreted within an atomic picture, and should be explained by taking account of the delocalization of $4d^9 4f^{n+1}$ excited states in compounds.

The purpose of the present study is to investigate decay processes of the $4d^9 nf^1$ ($n \geq 4$) excited states in the isoelectronic sequence from Cs^+ to La^{3+} by means of photoelectron spectroscopy. The investigation of nonradiative decay processes of $4d^9 4f^{n+1}$ states in rare earths has been extensively performed as a function of photon energies using the technique of resonant photoemission.[21,22] These studies show that such excited states decay nonradiatively through ordinary Auger processes and direct-recombination processes between a 4*d* hole and an excited 4*f* electron transferring the energy to an electron in the core level or the valence band. However, although much attention has been directed at the energy positions and density of states of the 4*f* level, the localization of the $4d^9 f^{n+1}$ excited states has scarcely been investigated. We choose the isoelectronic sequence of Cs, Ba, and La fluorides as samples to study systematic change of decay processes depending on the variation of the potential barrier. We measured the energy distribution curves (EDC's) of photoelectrons as well as constant-initial-state (CIS) spectra with initial states at the valence band and some core levels of cations and also measured constant-final-state (CFS) spectra with final states corresponding to the kinetic energy of the Auger electrons.

II. EXPERIMENTAL PROCEDURE

Photoelectron spectra were obtained with an ultrahigh-vacuum photoelectron spectrometer. Syn-

chrotron radiation from an electron-storage ring at the Institute for Solid State Physics of the University of Tokyo was used as a light source, and monochromatized with a 2-m grazing-incidence monochromator of a modified Rowland-mount type. The spectral width was about 0.18 eV at the photon energy of 90 eV with 100-μm entrance and 50-μm exit slits and a 1200-groove/mm grating. Energy distribution of photoelectrons was measured with a double-stage electrostatic energy analyzer of a cylindrical mirror type. The analyzer resolution was constant with a full width at half maximum of 0.4 eV.

Since charging of samples can result in shift and broadening of structures in the photoelectron spectrum, very thin films of CsF, BaF_2, and LaF_3 were prepared *in situ* by evaporation onto gold substrates. The thickness of samples was estimated to be about 100 Å with an oscillating-quartz thickness gauge.

The base pressure in a sample chamber was about 3×10^{-8} Pa and rose to the 10^{-6}-Pa range during evaporation. The pressure in an analyzer chamber was about 4×10^{-9} Pa during measurements. The spectral distribution of incident radiation was determined from a photoelectric yield spectrum of gold.

In the case of CIS measurements the retarding potential between samples and electron-energy analyzer was synchronously swept with the photon-energy scan of the monochromator. Also, CIS spectra were constructed from a set of photoelectron spectra excited at different photon energies. Good agreement was obtained in both CIS spectra.

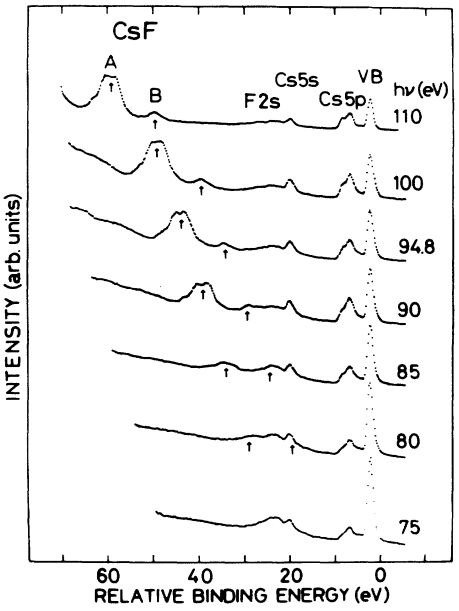

FIG. 1. Set of EDC's for CsF excited with photon energies around the Cs 4*d* excitation energy. The excitation photon energies ($h\nu$) are indicated on the right-hand side of each spectrum. Binding energies are given relative to the top of the valence band. Intensities are normalized to the incident photon flux. Two arrows indicate positions of constant kinetic energies.

III. RESULTS

Figure 1 shows a set of EDC's for CsF which were obtained with various photon energies around Cs 4*d* excitation energy. Excitation photon energies ($h\nu$) are indicated on the right-hand side of each spectrum. Binding energies are given relative to the top of the valence band. Ordinates are proportional to the number of photoelectrons per photon flux. EDC's of CsF have been measured by Poole *et al.*[25] and Smith and Pong[26] with helium- and hydrogen-discharge sources. The shape and width of the valence band and Cs 5*p* region are similar to those obtained by Poole *et al.*, but the intensity ratio of the $5p_{3/2}$ to $5p_{1/2}$ levels is different from the spectrum measured with an excitation energy of 23.1 eV by Smith and Pong.[26] In Fig. 1 the valence band as well as Cs $5p_{3/2,1/2}$, Cs 5*s*, and F 2*s* core levels are clearly seen. These are labeled for the spectrum taken at $h\nu=110$ eV. The measured binding energies for various states relative to the top of the valence band are listed in Table I. Two broad features labeled *A* and *B* for the spectrum taken at $h\nu=110$ eV are Cs-derived Auger transitions. The two arrows in each spectrum in Fig. 1 indicate positions of constant kinetic energies, respectively. Kinetic energies of the Auger electrons are also listed in Table I. These two Auger peaks show drastic change in intensity as the photon energy is changed around the Cs 4*d* threshold. The Cs 5*p* and 5*s* levels are also enhanced, while the valence band, which has mainly F 2*p* character, and F 2*s* level do not show any enhancement. These phenomena are more visual in CIS spectra with initial states at the peak of the valence band and Cs core levels and the CFS spectrum with the final state corresponding to the kinetic energy of Auger electron peak *A*. These are shown in Fig. 2 together with the total photoelectric yield (TY) spectrum.

As seen in Fig. 2 the TY spectrum of CsF shows many peaks and shoulders *A*–*K*. General features of structures and their energy positions in the present TY spectrum agree well with those in the Cs $N_{4,5}$ absorption spectrum of CsF measured by Cardona *et al.*[11] The CFS spectrum also shows peaks and shoulders labeled *A*–*K*. These energy positions agree well with peaks and shoul-

TABLE I. Binding energies of valence-band and core levels as well as the kinetic energies of Auger electrons observed in the spectra taken at $h\nu=115.0$, 120.5, and 130.0 eV for CsF, BaF_2, and LaF_3, respectively. Energies are given in eV relative to the top of the valence band. *R* represents the cation.

	CsF	BaF_2	LaF_3
R $4d_{3/2}$	73.9	87.2	102.0
R $4d_{5/2}$	71.4	84.5	99.2
F 2*s*	23.7		24.0
R 5*s*	19.9		31.0
R $5p_{1/2}$	8.2	11.2	15.8
R $5p_{3/2}$	7.2	9.5	13.2
VB peak	2.4	2.2	2.2
Auger feature *A*	50.8	59.5	64.0
Auger feature *B*	60.6	71.3	83.6

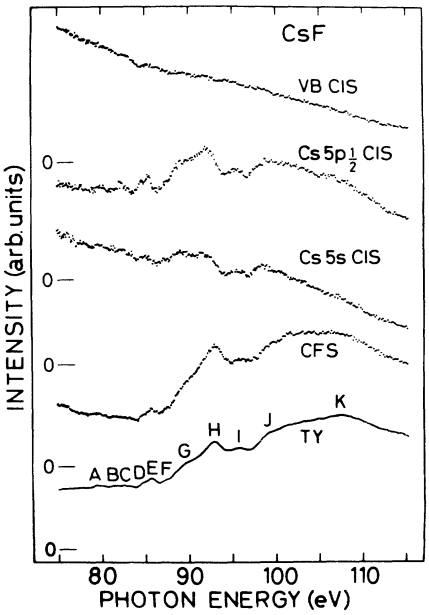

FIG. 2. Valence-band (VB) CIS, Cs $5p_{1/2}$ CIS, Cs 5s CIS, CFS, and TY spectra of CsF.

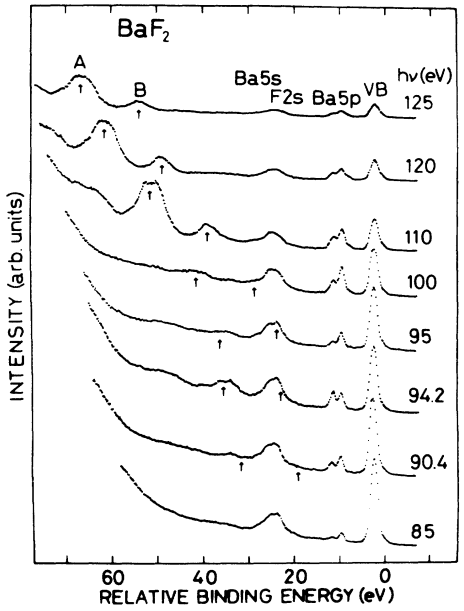

FIG. 3. Set of EDC's for BaF_2 excited with photon energies around the Ba 4d excitation energy. The excitation photon energies ($h\nu$) are indicated on the right-hand side of each spectrum. Binding energies are given relative to the top of the valence band. Intensities are normalized to the incident photon flux. Two arrows indicate positions of constant kinetic energies.

ders $A-K$ in the TY spectrum. The $5p_{1/2}$ CIS spectrum (CIS spectrum with the initial state at the peak of the Cs $5p_{1/2}$ level) shows peaks and shoulders, but structures above 90 eV locate at different energy positions from those in the CFS and TY spectra. The $5p_{1/2}$ CIS spectrum coincides well in shape and in energy with the $5p_{3/2}$ CIS spectrum (not shown). The 5s CIS spectrum also shows peaks at the same energy in the $5p_{1/2}$ CIS spectrum, but its intensity distribution is different from the $5p_{1/2}$ CIS spectrum. The intensity distributions of structures in the CFS and TY spectra agree with each other, while the shape of the 5s and $5p_{1/2}$ CIS spectra is much different from that of the CFS and TY spectra. The VB CIS spectrum (CIS spectrum with the initial state at the peak of the valence band) of CsF shows no enhancement and its intensity decreases monotonously with increasing photon energy.

Figure 3 shows a set of EDC's for BaF_2 with various photon energies around the Ba 4d threshold. In addition to the valence band, Ba $5p_{3/2,1/2}$ core levels are clearly seen, but unfortunately Ba 5s and F 2s levels overlap with each other. Two broad peaks labeled A and B in the spectrum taken at 125 eV are Ba-derived Auger transitions. The arrows in each spectrum in Fig. 3 indicate positions of constant kinetic energies, respectively. The measured binding energies for various states and kinetic energies of Auger electrons are listed in Table I. The intensity of the valence band decreases monotonously with increasing photon energy, while the two Auger peaks and Ba $5p_{1/2}$ and $5p_{3/2}$ core levels show drastic change in intensity and in shape as the photon energy is tuned through the absorption features shown at the bottom of Fig. 4.

Figure 4 shows CIS spectra with initial states at the peak of the valence band, Ba $5p_{3/2}$, and Ba $5p_{1/2}$ levels, the CFS spectrum with the final state corresponding to the kinetic energy of the Auger peak A, and the TY spectrum of BaF_2. Since the Ba 5s and F 2s levels overlap, the Ba 5s CIS spectrum was not measured. The TY spectrum shows two weak peaks and several intense structures on their high-energy side. Energy positions of structures in the present TY spectrum agree well with those obtained in the Ba $N_{4,5}$ absorption spectrum of BaF_2 measured by Miyahara *et al.*[14] In these structures

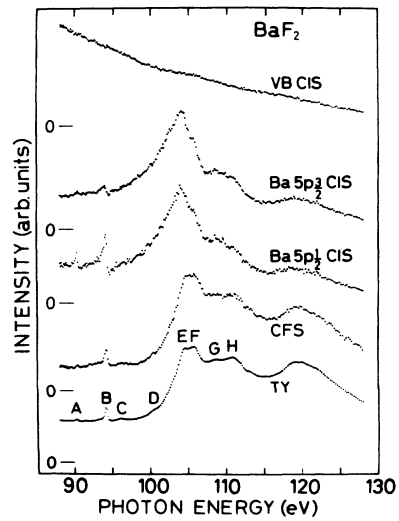

FIG. 4. Valence-band (VB) CIS, Ba $5p_{3/2}$ CIS, Ba $5p_{1/2}$ CIS, CFS, and TY spectra of BaF_2.

weak peaks A and B correspond to quasiatomic transitions for Ba^{2+} from the ground state $4d^{10}$ ($^1S_0$) to the excited states $4d^9 4f^1$ ($^3P_1$ and $^3D_1$, respectively).[14] According to Connerade and Mansfield,[27] the $4d \rightarrow 5f$ transitions possess significant oscillator strength and thus structures above 105 eV in the TY spectrum are associated with the $4d \rightarrow nf$ ($^1P_1$) transitions ($n \geq 5$) as well as the $4d \rightarrow 4f$ ($^1P_1$) transition. As seen in Fig. 4 the CFS spectrum of BaF_2 shows enchancement at respective absorption features, and the TY and CFS spectra closely resemble each other in shape. Ba $5p_{1/2}$ and $5p_{3/2}$ CIS spectra show resonant behavior, but the intensity distributions of both CIS spectra are different from each other, especially, at the excitation photon energy of the $^3D_1$ state, that is, the $5p_{1/2}$ CIS spectrum is more intense than the $5p_{3/2}$ CIS spectrum as seen in Fig. 3. Moreover, both of the $5p$ CIS spectra are different in shape from the CFS and TY spectra, and the position of the main peak E in the $5p$ CIS spectra is observed at the slightly lower-energy position than that in the TY spectrum. The VB CIS spectrum shows no enhancement around the Ba $4d$ threshold as shown in Fig. 4.

Figure 5 shows a set of EDC's for LaF_3 with various photon energies around the La $4d$ threshold. The valence band as well as the La $5p_{3/2,1/2}$, F $2s$, and La $5s$ core levels are clearly seen. Two broad peaks A and B are La-derived Auger transitions, and arrows indicate positions of constant kinetic energies of these Auger peaks at different excitation energies. The two Auger peaks show drastic change in intensity and in shape as photon energy is tuned through the absorption features shown at the bottom of Fig. 6. The La $5s$, La $5p_{1/2}$, and La $5p_{3/2}$ core

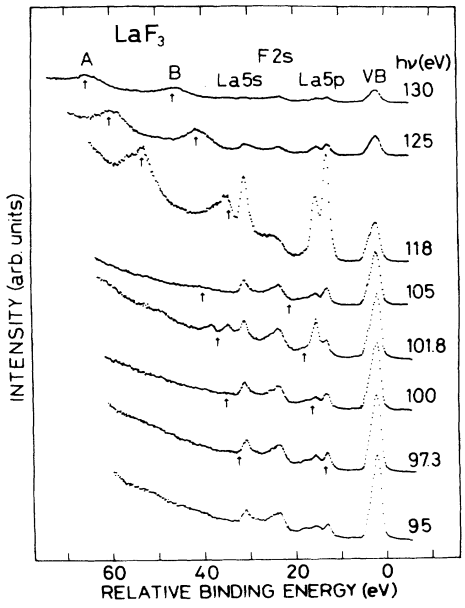

FIG. 5. Set of EDC's for LaF_3 excited with photon energies around the La $4d$ excitation energy. The excitation photon energies ($h\nu$) are indicated on the right-hand side of each spectrum. Binding energies are given relative to the top of the valence band. Intensities are normalized to the incident photon flux. Two arrows indicate positions of constant kinetic energies.

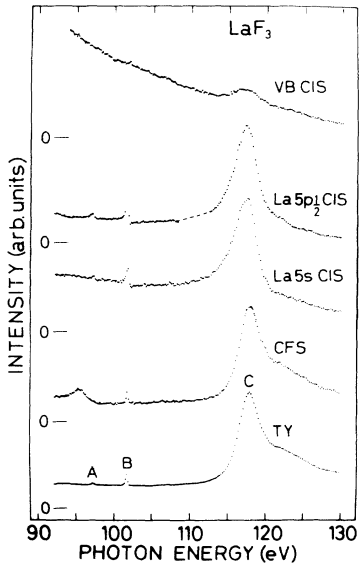

FIG. 6. Valance-band (VB) CIS, La $5p_{1/2}$ CIS, La $5s$ CIS, CFS, and TY spectra of LaF_3.

levels also show resonant enhancement at La $4d$ excitation, and the photoemission branching ratio of La $5p_{3/2}$ to $5p_{1/2}$ levels changes drastically at an excitation photon energy of 101.8 eV. This energy corresponds to the $^3D_1$ excitation. These phenomena have been observed in LaF_3 by Miller and Chiang[23] and in LaB_6 by Aono *et al.*[24] The change in the kinetic energy of the Auger electron near the ionization threshold has been interpreted in terms of postcollision interaction and the change of the shape of Auger peak A at $^3D_1$ excitation energy has been interpreted in terms of formation of the ^1P and ^3P Auger final states.[23] However, the change of the photoemission branching ratio of La $5p_{3/2}$ to $5p_{1/2}$ levels is still an open question.

Figure 6 shows CIS spectra with initial states at the peak of the valence band, and La $5s$ and $5p_{1/2}$ levels, the CFS spectrum with the final state corresponding to the kinetic energy of the Auger electron peak A in Fig. 5, and the TY spectrum of LaF_3. Energy positions of structures in the present TY spectrum agree with those observed in the $N_{4,5}$ absorption spectrum measured by Suzuki, Ishii, and Sagawa.[7] However, there are some differences between them in intensity distribution at a higher-energy shoulder around 122 eV. The TY spectrum shows two weak peaks (A and B) and a giant peak (C). These peaks A, B, and C correspond to quasiatomic transitions for La^{3+} from the ground state to the $4d^9 4f^1$ excited states $^3P_1$, $^3D_1$, and $^1P_1$, respectively. The CFS spectrum also shows the peaks corresponding to $^3D_1$ and $^1P_1$ states, but the $^3P_1$ peak is obscure because of overlapping of the La $5s$ peak at $h\nu = 95.5$ eV. Except for this peak, the positions and the intensity distribution of the peaks in the CFS spectrum agree well with those in the TY spectrum. The $5p_{1/2}$ CIS spectrum shows enhancement as the photon energy is tuned though the absorption features, but positions of peaks are slightly different from those observed in the TY spectrum. For instance,

the peak C in the TY spectrum locates at 117.8 eV, while that in the La $5p_{1/2}$ CIS spectrum is 117.3 eV. Moreover, the intensity distribution of the $5p_{1/2}$ CIS spectrum is quite different from that of the TY spectrum, especially at the $^3D_1$ excitation energy. The VB CIS spectrum of LaF_3 shows a broad peak at about 117 eV in contrast to the cases of CsF and BaF_2.

IV. DISCUSSION

A. Direct-recombination processes

As seen in Figs. 1–6, the enhancement of 5s and 5p levels of cations is clearly observed for all samples investigated here (the Ba 5s level is not clear due to the overlap with the F 2s level) as the photon energy is tuned through the absorption features. This enhancement can be interpreted in terms of the nonradiative decay of 4d-hole states of cations, where a 4d hole and an excited electron recombine directly with the energy transferred to a 5s electron or a 5p electron of cation. Here, we call these direct-recombination processes the "$N_{4,5}O_1$ process" or "$N_{4,5}O_{2,3}$ process", where $N_{4,5}$ denotes initial 4d-hole states and O_1 and $O_{2,3}$ denote final hole states. The final state of these decay processes has a hole in the 5s or 5p level and an electron in the continuum. Since these configurations are the same as those of the direct photoexcitations from the 5s level or the 5p level, the decay of 4d-hole states through the $N_{4,5}O_1$ or $N_{4,5}O_{2,3}$ process is observed as the resonant enhancement of the 5s level or the 5p level.

Theoretical absorption spectra for Xe-like ions in the region of 4d excitation have been calculated with use of a term-dependent Hartree-Fock technique and relativistic random-phase approximation.[18,19] For neutral Xe, the shape resonance in the ^1P channel leads to a giant peak in the spectrum above the 4d threshold. As this shape resonance gradually moves below the ionization limits with increasing nuclear charge, interactions with nf levels are enhanced, resulting in the hybridization of nf wave functions and relatively large oscillator strength for the discrete $4d \rightarrow nf\ ^1P$ transitions.[18] Thus the $4d \rightarrow nf\ ^1P$ transitions may correspond to structures up to 95 eV in CsF and to about 110 eV in BaF_2, though the spectral feature of the BaF_2 and Ba^{2+} free ions[13] is entirely different from each other. This difference may be caused by the difference between solid and free ion samples. In the case of LaF_3, the $4d \rightarrow 4f\ ^1P$ transition appears at about 118 eV and transitions to higher nf levels ($n \geq 5$) may situate above 120 eV.

It is noticed that the energy region of the enhancement of 5s and 5p CIS spectra roughly coincides with the region where giant peaks are observed in the TY spectra. However, the degree of the enhancement of CIS spectra is suppressed in the energy region above the first giant peak (peaks H, E, and C for CsF, BaF_2 and LaF_3, respectively), and the enhanced region seems to become narrower with going from CsF to LaF_3. These observations suggest that the $4d^9f^1$ excited states in CsF and BaF_2 can decay through the $N_{4,5}O_1$ and $N_{4,5}O_{2,3}$ processes even though they are higher nf states ($n \geq 5$). In the case of LaF_3, however, higher nf states decay scarcely through the direct-recombination processes and decay mainly through the Auger processes. These results may relate the collapse of the potential barrier along the isoelectronic sequence.

The main peak in the CIS spectra is observed on the lower-energy side (0.5–0.8 eV) than that observed in respective TY spectra. Similar energy shift has been observed in the $N_{4,5}$ emission spectra of LaB_6, where the radiative decay from the $4d^94f^1$ ($^3P_1$, $^3D_1$, and $^1P_1$) excited states to the ground state is clearly observed.[28] The $^3P_1$ and $^3D_1$ emission lines in the $N_{4,5}$ emission spectrum are located at the same energy positions as those observed in the absorption spectrum, while the $^1P_1$ emission peak is observed at about 0.5 eV below the absorption peak. These results agree well with the present CIS spectra of BaF_2 and LaF_3 and suggest that an electron excited from the 4d level to the $^1P_1$ ($4d^95f^1$) state of higher-energy states decays scarcely through the direct-recombination process both radiatively and nonradiatively. In other words, a 4f electron excited below energy states of the $^1P_1$ absorption peak interacts strongly with a 4d hole and easily causes the direct-recombination decay, while the 4d-f interaction is not so strong to a 4f electron excited above the absorption peak C and causes autoionization to the continuum.

It is worthwhile to note that the VB CIS spectrum of LaF_3 shows enhancement around the $^1P_1$ excitation energy, but those of CsF and BaF_2 show no enhancement. These results indicate that there is no interaction between valence states and 4d excited states in CsF and BaF_2, but valence states of LaF_3 interact with $4d^94f^1$ excited states to some extent. Thus valence states, which are mainly composed of F 2p character, may localize tightly around the F^- ion in CsF and BaF_2, while valence states of LaF_3 may extend to the vicinity of the La^{3+} ion.

B. Auger decay processes

As seen in Figs. 1, 3, and 5, two Auger peaks are observed for CsF, BaF_2, and LaF_3. Their kinetic energies increase systematically with increasing atomic number of the cation. Thus these Auger peaks may originate from the same transitions in the cation site among CsF, BaF_2, and LaF_3. Auger peaks corresponding to the present ones have been observed for LaF_3 (Ref. 23) and LaB_6.[24] Aono *et al.*[24] have stated that features A and B are derived from La $N_{4,5}O_1V$ and $N_{4,5}O_{2,3}V$ Auger transitions, respectively, because the valence band of LaB_6 extends widely in the crystal. In the case of LaF_3, however, Miller and Chiang have attributed feature A in Fig. 5 to the $N_{4,5}O_1O_{2,3}$ Auger transition, because LaF_3 is ionic and the valence electrons locate around the F^- ion.[23] However, it is noticed that the kinetic energy of the $N_{4,5}O_1O_{2,3}$ Auger should be less than 55 eV for LaF_3 from measurements of kinetic energies of Auger electrons and binding energies of core levels concerned. This value does not include correlation energy of the remaining two holes in the final state of the Auger transition. On the

other hand, the measured kinetic energy (relative to the top of the valence band) of feature A is about 64 eV. Thus we think that feature A corresponds to the $N_{4,5}O_{2,3}O_{2,3}$ Auger transition.

The other Auger feature B is always less intense than feature A, but it is somewhat intense in LaF_3 compared with the cases of CsF and BaF_2. This may correspond to the observations in which the VB CIS spectrum of LaF_3 shows enhancement in contrast to the cases of CsF and BaF_2 as mentioned in the preceding section. This result implies that the overlap between wave functions of the $4d$-hole state and the valence band is somewhat larger in LaF_3 than those in CsF and BaF_2. In other words the valence states of LaF_3 delocalize compared with those of CsF and BaF_2. We have investigated nonradiative decay processes of core excitons in alkali halides[29–31] and magnesium halides.[32] These substances, NaF and MgF_2, show dip or no enhancement in the VB CIS spectra due to the direct-recombination process of the $2p$ core exciton as the excitation photon energy is tuned through the excitation energy of the core exciton, but the $L_{2,3}VV$ Auger transition is clearly observed. These phenomena may apply in the present case. Thus we attribute feature B to the $N_{4,5}O_{2,3}V$ Auger transition even though the enhancement of the valence-band spectra is not observed for CsF and BaF_2.

The $4d$-hole states created by photoabsorption decay through the $N_{4,5}O_{2,3}O_{2,3}$ and $N_{4,5}O_{2,3}V$ Auger processes which show enhancement in CFS spectra with the final states corresponding to the kinetic energy of each Auger electron. We call these Auger decay processes the "$N_{4,5}O_{2,3}O_{2,3}$ process" or "$N_{4,5}O_{2,3}V$ process." The final state of the $N_{4,5}O_{2,3}O_{2,3}$ process involves two holes in the $5p$ level and an electron in the continuum. We have observed that the kinetic energy of the Auger electron, which is caused by the decay of the core exciton through the Auger process, is slightly larger than that of the ordinary Auger electron measured at excitation photon energy far above the threshold.[29–32] The reason for this energy gain has been attributed to the formation of a bound state involving two holes in the valence band and an electron which formed a core exciton.

In the cases of CsF and BaF_2, the kinetic energy of the $N_{4,5}O_{2,3}O_{2,3}$ Auger electron is essentially constant within the resolution of the electron-energy analyzer (0.4 eV) in the entire excitation energy region measured here. However, the $N_{4,5}O_{2,3}O_{2,3}$ Auger peak of LaF_3 shifts to lower and higher energies at excitation energies of $^1P_1$ and $^3D_1$ states, respectively, compared with the case of the other excitation energies. Moreover, its shape changes at the $^3D_1$ excitation. Since the $^3D_1$ state locates below the $4d$ ionization threshold, an excited $4f$ electron may still be bound during the $N_{4,5}O_{2,3}O_{2,3}$ process. Thus an excited $4f$ electron may couple with two holes in the $5p$ level and form a bound state so that the system becomes stable when the Auger transition occurs. This coupling produces an upward shift of the kinetic energy of the Auger electron at the $^3D_1$ excitation.

The $^1P_1$ state situates far above the $4d$ threshold and can easily autoionize to the continuum. When the $N_{4,5}O_{2,3}O_{2,3}$ Auger transition occurs in this circumstance, the remaining two holes in the $5p$ level strongly attract an ejected Auger electron and a free electron decoupled with a $4d$ hole may not participate in the shielding against the attractive force produced by the two holes. Therefore the Auger electron at the $^1P_1$ excitation has a smaller kinetic energy than that observed with the other excitation energy. The change in Auger shape in LaF_3 as photon energy increases from 118 to 130 eV is mainly due to changes in the $4d_{5/2}$-$4d_{3/2}$ photoemission branching ratio as suggested by Miller and Chiang.[23]

In the cases of CsF and BaF_2, the overlap of the $4f$ orbit with the $4d$ orbit is not so excellent compared with that in LaF_3, because the centrifugal potential barrier separating inner and outer wells for nf ($n=4,5,\ldots$) orbits is not so high.[18,19] Thus the $4d^9 4f^1$ states in CsF and BaF_2 produced by photoabsorption delocalize compared with that in LaF_3 so that the kinetic energy and the shape of the $N_{4,5}O_{2,3}O_{2,3}$ Auger transition do not change in the entire excitation energy region measured here.

It is noted that the CFS spectra with the final state corresponding to the kinetic energy of the $N_{4,5}O_{2,3}O_{2,3}$ Auger electron agree well in shape and in energy position of their structures with the respective TY spectra. On the other hand, the CIS spectra are different in shape from the respective TY spectra. This implies that $4d$ excited states decay dominantly through the $N_{4,5}O_{2,3}O_{2,3}$ process and the decay probability of this process is almost constant in the energy region concerned here.

C. Change of branching ratio of $5p_{3/2}$ to $5p_{1/2}$ levels in BaF_2 and LaF_3

Figure 7 shows a set of EDC's for LaF_3 in the region of $5p$ levels and valence band in more detail. Ordinates are

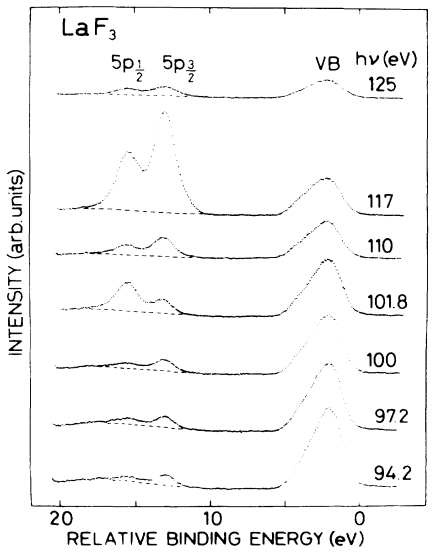

FIG. 7. Set of EDC's for LaF_3 excited with photon energies around the La $4d$ excitation energy. The excitation photon energies ($h\nu$) are indicated on the right-hand side of each spectrum. Binding energies are given relative to the top of the valence band. Intensities are normalized to the incident photon flux. Dashed lines denote the background.

proportional to the number of photoelectrons per photon flux. Intensities of $5p_{1/2}$ and $5p_{3/2}$ peaks show drastic change and their ratio also changes drastically at the excitation energy of the $^3D_1$ state (101.8 eV). On the other hand, the photoemission branching ratio of $5p_{3/2}$ to $5p_{1/2}$ levels is almost constant at excitation energies of the $^3P_1$ (94.2 eV) and $^1P_1$ (117 eV) states. These changes in branching ratio are more visual in Fig. 8. Figure 8 shows the excitation energy dependence of photoemission branching ratios of $5p_{3/2}$ to $5p_{1/2}$ levels in BaF_2 and LaF_3. Closed and open circles represent the ratios for BaF_2 and LaF_3, respectively. Arrows in this figure denote the excitation energies of the $^3D_1$ state of BaF_2 and LaF_3. These branching ratios are obtained from the peak intensity of $5p_{1/2}$ and $5p_{3/2}$ levels after subtracting the background from the spectra as shown by dashed lines in Fig. 7. As shown in Fig. 8, the photoemission branching ratio of $5p_{3/2}$ to $5p_{1/2}$ levels changes drastically and deviates from a statistical value as the photon energy is across the excitation energy of the $^3D_1$ state. For example, the ratio of the Ba $5p_{3/2}$ to $5p_{1/2}$ levels is about 1.7 at an excitation photon energy of 90 eV, while at the $^3D_1$ excitation energy it is about 0.93. In the case of LaF_3, the ratio is 0.27 at the $^3D_1$ excitation energy and ranges from 1.3 to 1.8 at the other excitation energies. Although the $N_{4,5}O_{2,3}V$ Auger peak locates near the $5p$ peak of LaF_3 at the excitation energy of the $^3D_1$ state, the Auger peak in BaF_2 locates far from the $5p$ peak at the $^3D_1$ excitation energy. Moreover, the intensity of this Auger peak is weak at the $^3D_1$ excitation energy. Thus the anomaly of the branching ratio is not due to the overlap of the Auger peak and is essentially caused by the decay process of the $^3D_1$ state.

Let us see the line shape of $5p_{3/2}$ and $5p_{1/2}$ CIS spectra of LaF_3 in detail at excitation photon energies around $^3P_1$ and $^3D_1$ states. These are shown in Fig. 9 together with the TY spectrum. It is noticed that the intensity ratios of the $^3P_1$ and $^3D_1$ peaks are different between the $5p_{3/2}$ and $5p_{1/2}$ CIS spectra. Moreover, line shape of the $^3D_1$ peak

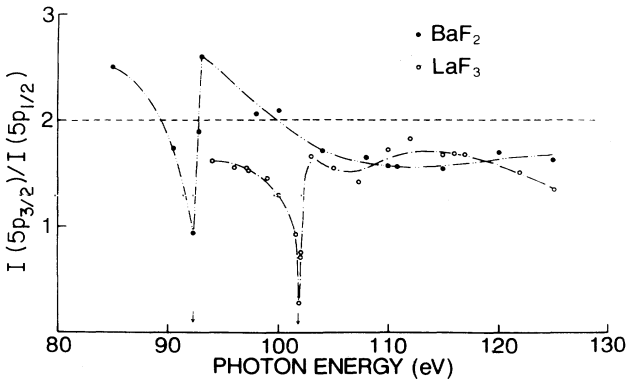

FIG. 8. Excitation photon-energy dependence of photoemission branching ratios of $5p_{3/2}$ to $5p_{1/2}$ levels in BaF_2 and LaF_3. Closed and open circles represent the ratios for BaF_2 and LaF_3, respectively. Arrows denote excitation energies of the $^3D_1$ state of BaF_2 and LaF_3. Horizontal dashed line denotes expected branching ratio from statistical degeneracy.

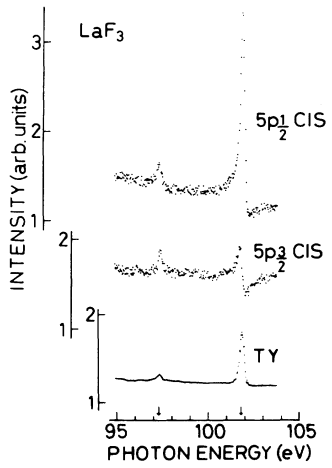

FIG. 9. La $5p_{3/2}$ CIS, La $5p_{1/2}$ CIS, and TY spectra of LaF_3.

in the CIS spectra shows Fano-resonance behavior, whereas the $^3P_1$ peak has almost symmetrical shape. These results suggest that the $^3D_1$ state interacts strongly with the continuum when a $4d$ hole annihilates through $N_{4,5}O_2$ and $N_{4,5}O_3$ processes, and this interaction may cause the change of the branching ratio. On the other hand, the $^3P_1$ state seems to interact scarcely with the continuum compared with the $^3D_1$ state, and the branching ratio of the $5p_{3/2}$ and $5p_{1/2}$ levels is kept almost the same value at the excitation photon energy far from the $4d$ threshold.

Anomalous behavior of the branching ratio has been observed in many samples and explained by the "final-state model."[33–40] In this model it is assumed that both spin-orbit components have the same photoionization cross section per electron for excitation to a given final state. Thus the abrupt change in absorption coefficient in the energy region comparable to the spin-orbit splitting causes the change of the branching ratio as the excitation photon energy is tuned through the sharp absorption structure, because the initial core levels in question are separated by the spin-orbit interaction. If this is the case, the branching ratio should change at the excitation photon energy of the $^3P_1$ state, too. However, it seems to be almost constant at that energy. Thus the present results cannot be explained by the final-state model.

The other mechanism of the change of the branching ratio of the spin-orbit pair has been observed in absorption spectra of the exciton for ionic crystals.[31,41–44] For example, Na $L_{2,3}$ absorption spectra of sodium halides show two peaks corresponding to the L_2 and L_3 core excitons, and branching ratios of L_3 to L_2 exciton peaks range from 0.15 to 0.3 although the expected value from the statistical degeneracy of L_2 and L_3 is 2. This difference has been explained by Onodera and Toyozawa[45] with an intermediate coupling scheme. If the spin-orbit splitting of the Na $2p$ level and the energy of the exchange interaction between an electron and a hole which form the exciton are comparable, the branching ratio of the L_3 to L_2 core excitons should deviate from the expected value. In the present case, however, the sit-

uation is more complicated than the case of excitons, because the system involves the decay of the $^3D_1$ state through the $N_{4,5}O_{2,3}$ process.

LaGraffe, Dowben, and Onellion[46] have observed the magnetic ordering of thin Tb overlayers by measuring the Tb $5p_{3/2}$ to $5p_{1/2}$ branching ratio above and below the Tb Curie temperature. According to LaGraffe, Dowben, and Onellion the eigenfunctions of the $p_{3/2}$ level, $m_j=\pm\frac{3}{2}$ are of well-defined spin character, while the $p_{1/2}$ and $p_{3/2}$, $m_j=\pm\frac{1}{2}$ eigenfunctions are of mixed spin character. As a result of these differences in the $5p$ initial state, there are differences, in the final state, in the interaction between $5d$ valence states and $5p$ core levels. This $5d$-$5p$ coupling causes a change in the light polarization as a result of the changing symmetry selection rules in photoemission.[46] This occurs even without alignment of the spatial coordinate system with the magnetic coordinate system. A similar result has been found for Gd overlayers on Cu(100).[47,48]

Because of the symmetry restrictions upon the final state, the ion left after a photoemission event must have a symmetry similar to the orbit from which the photoelectron was ejected. The total symmetry requirement is satisfied by coupling with the wave function of the outgoing electron. This symmetry restriction requires that photoemission from the $5p$ level can yield an s-like and a d-like wave, but the symmetry of the resulting ion must be $^3D_1$ in the present case, because the $5p$ CIS spectra show the resonant behavior at the excitation photon energy of the $^3D_1$ state as mentioned above. This suggests that the outgoing wave is d-like, and a $5p_{1/2}$ hole and a $d_{3/2}$ electron may produce $^3D_1$ state coupling with each other in the final state. This coupling causes unusual anomaly of the photoemission branching ratio of $5p_{3/2}$ to $5p_{1/2}$ levels in BaF_2 and LaF_3 as the excitation photon energy is tuned through the excitation energy of the $^3D_1$ ($4d^9 4f^1$) state.

Recently Ogasawara, Thole, and Kotani[49] have calculated the photoemission branching ratio of La $5p_{3/2}$ to $5p_{1/2}$ levels including the $N_{4,5}O_{2,3}$ process with an atomic picture. Their results show that the branching ratio is very sensitive to the excitation photon energy and the La $5p_{1/2}$ peak becomes more intense than the $5p_{3/2}$ at the excitation energy of the ^3D state, whereas it keeps almost the same value as a statistical value at ^1P and ^3P excitations. These calculated results explain our experimental results well. The difference between the branching ratios in BaF_2 and LaF_3 may be caused by the difference in the degree of mixing between d states and other states at high-energy continuum in both materials. However, further theoretical investigations are desired to interpret quantitatively the difference between the branching ratios in BaF_2 and LaF_3.

V. CONCLUSION

The nonradiative decay of $4d$ hole states in CsF, BaF_2, and LaF_3 are investigated by measuring EDC's of photoelectrons as well as CIS spectra with initial states at the valence band and some core levels and CFS spectra with final states corresponding to the kinetic energy of Auger electrons. It is observed that the $N_{4,5}O_{2,3}O_{2,3}$ Auger peak is resonantly enhanced around the energy region of $4d$ excitation of cations. The CFS spectra with the final state at this Auger electron are in good agreement in shape and in energy with respective absorption features. Intensities of $5s$ and $5p$ electrons of cations are also resonantly enhanced due to the direct-recombination processes between a $4d$ hole and an excited electron transferring the energy to an electron in the $5s$ level or the $5p$ level, while the valence band does not show any enhancement except for LaF_3. The spectral shape of the $5s$ and $5p$ CIS spectra is different from the absorption features. Especially, the intensity of the CIS spectra in the higher-energy region decreases rapidly with increasing photon energy compared with respective TY spectra. From these results, the $4d$-hole states decay dominantly through the $N_{4,5}O_{2,3}O_{2,3}$ process and the direct-recombination processes are suppressed in the energy region above the first giant absorption feature. The valence states of CsF and BaF_2 localize around the F^- ion so that valence-band CIS spectra cannot enhance due to the direct-recombination prcoess of $4d$-hole states, while that of LaF_3 is delocalized. It is also found that the photoemission branching ratio of $5p_{3/2}$ to $5p_{1/2}$ levels of BaF_2 and LaF_3 changes drastically as the excitation photon energy is tuned across the excitation energy of the $^3D_1$ state. It is attributed to the difference in the p-d interaction between $5p_{1/2}$ and $5p_{3/2}$ hole states at the final state of photoemission.

ACKNOWLEDGMENTS

The authors very much appreciated the support by the staff of the Synchrotron Radiation Laboratory of the Institute for Solid State Physics of the University of Tokyo during measurements.

[1]T. M. Zimkina, V. A. Fomichev, S. A. Gribovskii, and I. I. Zhukova, Fiz. Tverd. Tela (Leningrad) 9, 1447 (1967) [Sov. Phys.—Solid State 9, 1128 (1967)].

[2]V. A. Fomichev, T. M. Zimkina, S. A. Gribovskii, and I. I. Zhukova, Fiz. Tverd. Tela (Leningrad) 9, 1490 (1967) [Sov. Phys.—Solid State 9, 1163 (1967)].

[3]R. Haensel, P. Rabe, and B. Sonntag, Solid State Commun. 8, 1845 (1970).

[4]S. Suzuki, I. Nagakura, T. Ishii, T. Satoh, and T. Sagawa, Phys. Lett. 41A, 95 (1972).

[5]V. F. Demekhin, Fiz. Tverd. Tela (Leningrad) 16, 1020 (1974) [Sov. Phys.—Solid State 16, 659 (1974)].

[6]D. W. Lynch and C. G. Olsen, in *Proceedings of the IV International Conference on Vacuum Ultraviolet Radiation Physics, Hamburg (1974)*, edited by E. E. Koch, R. Haensel, and C. Kunz (Pergamon/Vieweg, Braunschweig, 1974), p. 258.

[7]S. Suzuki, T. Ishii, and T. Sagawa, J. Phys. Soc. Jpn. 38, 156 (1975).

[8]M. Cukier, P. Dhez, and P. Jaeglé (unpublished).
[9]H. W. Wolff, R. Bruhn, K. Radler, and B. Sonntag, Phys. Lett. **59A**, 67 (1976).
[10]O. Aita, K. Ichikawa, M. Kamada, M. Okusawa, H. Nakamura, and K. Tsutsumi, J. Phys. Soc. Jpn. **56**, 649 (1987).
[11]M. Cardona, R. Haensel, D. W. Lynch, and B. Sonntag, Phys. Rev. B **2**, 1117 (1970).
[12]P. Rabe, K. Radler, and H.-W. Wolff, in *Proceedings of the IV International Conference on Vacuum Ultraviolet Radiation Physics, Hamburg (1974)*, edited by E. E. Koch, R. Haensel, and C. Kunz (Pergamon/Vieweg, Braunschweig, 1974), p. 247.
[13]T. B. Lucatorto, T. J. McIlath, J. Sugar, and S. M. Younger, Phys. Rev. Lett. **47**, 1124 (1981).
[14]T. Miyahara, T. Hanyu, H. Ishii, M. Yanagihara, T. Kamada, H. Kato, K. Naito, and S. Suzuki, J. Phys. Soc. Jpn. **55**, 408 (1986).
[15]J. L. Dehmer, A. F. Starace, U. Fano, J. Sugar, and J. W. Cooper, Phys. Rev. Lett. **26**, 1521 (1971).
[16]A. F. Starace, Phys. Rev. B **5**, 1773 (1972).
[17]J. Sugar, Phys. Rev. B **5**, 1785 (1972).
[18]K. T. Cheng and C. Froese Fischer, Phys. Rev. A **28**, 2811 (1983).
[19]K. T. Cheng and W. R. Johnson, Phys. Rev. A **28**, 2820 (1983).
[20]T. Jo, J. Phys. Soc. Jpn. **58**, 1452 (1989).
[21]J. W. Allen, S. J. Oh, O. Gunnarsson, K. Schönhammer, M. B. Maple, M. S. Torikachvili, and I. Lindau, Adv. Phys. **35**, 275 (1986).
[22]T. Ishii, K. Soda, K. Naito, T. Miyahara, H. Kato, S. Sato, T. Mori, M. Taniguchi, A. Kakizaki, Y. Ōnuki, and T. Komatsubara, Phys. Scr. **35**, 603 (1987).
[23]T. Miller and T.-C. Chiang, Phys. Rev. B **29**, 1121 (1984).
[24]M. Aono, T.-C. Chiang, J. A. Knapp, T. Tanaka, and D. E. Eastman, Phys. Rev. B **21**, 2661 (1980).
[25]R. T. Poole, J. G. Jenkin, J. Liesegang, and R. C. G. Leckey, Phys. Rev. B **11**, 5179 (1975).
[26]J. A. Smith and W. Pong, Phys. Rev. B **12**, 5931 (1975).
[27]J. P. Connerade and M. W. D. Mansfield, Phys. Rev. Lett. **48**, 131 (1982).
[28]K. Ichikawa, A. Nisawa, and K. Tsutsumi, Phys. Rev. B **34**, 6690 (1986).
[29]M. Kamada, K. Ichikawa, and K. Tsutsumi, Phys. Rev. B **28**, 7225 (1983).
[30]K. Ichikawa, M. Kamada, O. Aita, and K. Tsutsumi, Phys. Rev. B **32**, 8293 (1985).
[31]M. Kamada, O. Aita, K. Ichikawa, and K. Tsutsumi, Phys. Rev. B **36**, 4962 (1987).
[32]O. Aita, K. Ichikawa, and K. Tsutsumi, Phys. Rev. B **39**, 10 266 (1989).
[33]T. E. H. Walker, J. Berkowitz, J. L. Dehmer, and J. T. Waber, Phys. Rev. Lett. **31**, 678 (1973).
[34]J. L. Dehmer and J. Berkowitz, Phys. Rev. A **10**, 484 (1974).
[35]J. E. Rowe and G. Margaritondo, Phys. Lett. **57A**, 314 (1976).
[36]F. Wuilleumier, M. Y. Adam, P. Dhez, N. Sandner, V. Schmidt, and W. Mehlhorn, Phys. Rev. A **16**, 646 (1977).
[37]G. M. Bancroft, W. Gudat, and D. E. Eastman, Phys. Rev. B **17**, 4499 (1978).
[38]G. Margaritondo, J. E. Rowe, and S. B. Christman, Phys. Rev. B **19**, 2850 (1979).
[39]G. Margaritondo, F. Cerrina, G. P. Williams, and G. J. Lapeyre, J. Vac. Sci. Technol. **16**, 507 (1979).
[40]G. Margaritondo, R. Rosei, J. H. Weaver, and W. H. Becker, Solid State Commun. **34**, 401 (1980).
[41]J. E. Eby, K. J. Teegarden, and D. B. Dutton, Phys. Rev. **116**, 1099 (1959).
[42]K. Teegarden and G. Baldini, Phys. Rev. **155**, 896 (1967).
[43]S. Nakai and T. Sagawa, J. Phys. Soc. Jpn. **26**, 1427 (1969).
[44]S. Nakai, T. Ishii, and T. Sagawa, J. Phys. Soc. Jpn. **30**, 428 (1971).
[45]Y. Onodera and Y. Toyozawa, J. Phys. Soc. Jpn. **22**, 833 (1967).
[46]D. LaGraffe, P. A. Dowben, and M. Onellion, Phys. Lett. A **147**, 240 (1990).
[47]P. A. Dowben, D. LaGraffe, and M. Onellion, J. Phys. C **1**, 6571 (1989).
[48]D. LaGraffe, P. A. Dowben, and M. Onellion, Phys. Rev. B **40**, 970 (1989).
[49]H. Ogasawara, B. T. Thole, and A. Kotani (private communication).